*Bruno Andò, Salvatore Baglio, A.R. Bulsara, and Vincenzo Sacco*

# RTD Fluxgate: A Low-Power Nonlinear Device to Sense Weak Magnetic Fields

Fluxgate magnetometers have always been of interest to technical and scientific communities to sense weak magnetic fields (in the range of $10^{-6}$) with a resolution of 100 pT at room temperature. These devices find applicability in fields such as space, geophysical exploration and mapping, nondestructive testing, and assorted military applications. Very good examples of past and emerging applications of fluxgate magnetometers can be found in [14] and [20]. Fluxgates used in immunoassay techniques, as competitors of SQUID magnetometers [10], require even higher resolution (down to 10 pT) but may tolerate tighter operating ranges. Alternative technologies, based on anisotropic magnetoresistance, giant magnetoresistance, and magneto-impedance effects have also been recently studied in the context of precise magnetometers. Fluxgate systems prevail over these competitive technologies not only because of their higher sensitivity but also because of their lower noise level, robustness, and remarkable thermal and long-term stability.

Conventional fluxgate magnetometers use two excitation coils and two detection coils wound on two ferromagnetic cores and connected in a differential arrangement, as depicted in Figure 1 [5], [17]. By driving the excitation coils with two periodic counter-phased currents, the magnetic cores (which possess a bistable characteristic) are periodically driven into saturation in opposing ways.

The signals $V_i(t)$, $(i = 1, 2)$, at each detection coil oscillate at the frequency of the forcing term, with the output voltage signal denoted by $V(t) = V_1(t) - V_2(t)$ being zero, and an external (or target) magnetic field absent. The presence of an external magnetic field $H_x$ (dc or low frequency) leads to asymmetry in the core magnetization, leading to the appearance of odd and even harmonics of the drive frequency in the output power spectral density; the output signal $V_{\text{out}}(t)$, for measurement purposes, is extracted from the spectral amplitude of the second harmonic which is correlated with the level of the external magnetic field [11], [18].

Note that in the absence of the target signal, the power spectrum density (PSD) contains only the odd harmonics of the bias frequency. This readout scheme has some drawbacks; chief among them is the requirement of a large amount of onboard power to provide a high amplitude and high frequency excitation signal.

A new way to operate fluxgate magnetometers is represented by the residence times difference (RTD) fluxgate. Before exploring the potentiality of the RTD fluxgate, it will be useful to introduce some information about the intrinsic nonlinear behavior of this class of devices.

The scientific community is profoundly interested in exploiting the nonlinear properties of hysteretic devices, and applications in measurement systems are being thoroughly investigated. Great effort has been dedicated to developing theoretical formalizations describing the dynamic behavior of these systems, such as the state-space model, the viscoelastic model, the Preisach model, and potential-based models. [4], [7], [13], [19], [21].

There is no complete agreement on the use of the term hysteresis among the various research fields where memory effects are present. The term hysteresis is usually adopted to describe a rate-independent memory effect, although some works use this term to describe the dynamic behavior of

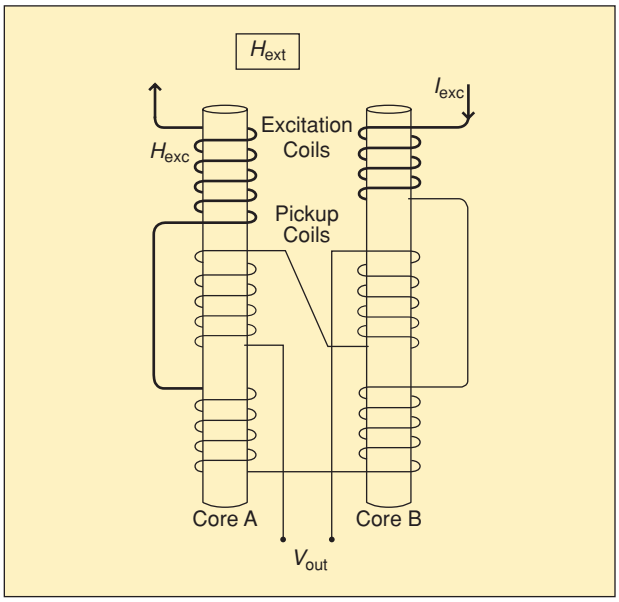


*Fig. 1.* Conventional arrangement for a traditional fluxgate magnetometer.


1094-6969/05/$20.00©2005IEEE

classes of materials and others use to distinguish between static hysteresis and dynamic hysteresis.

Although the two effects often coexist, the rate-dependent memory effect dominates at high frequencies due to the phase-lag effect. The rate-independent memory effect on the contrary prevails at low frequencies. To describe the behavior of dynamic hysteretic systems the Landau-Khalatnikov equation [7], [21] can be used, which, in the case of magnetic systems becomes

$$\tau \frac{dm}{dt} = -\frac{\partial U(m,t)}{\partial m}, \tag{1}$$

where $m$ is the magnetization and $\tau$ is the system time constant.

This model describes hysteretic behavior by using the energy function $U(m, t)$ ruling the switching mechanism between the two stable states of the system. The potential energy function is depicted in Figure 2(a) and described by

$$U(m, t) = \frac{m^2}{2} - c^{-1} \ln \cosh(c(m + H(t))) \tag{2}$$

where

- $c$ is a nonlinearity parameter (inversely proportional to the temperature), which controls the topology of the potential: the system becomes monostable, or paramagnetic, when $c < 1$, corresponding to an increase in the core temperature past the Curie point
- $H(t)$ is an external signal comprising the time-periodic (sinusoidal or triangular) reference signal ($H_e$) as well as the target signal ($H_x$) (taken to be dc throughout this treatment)
- the height of the potential barrier represents the energy required to switch from one state to the other.

The time constant $\tau$ in (1) rules the dynamic behavior of the system. If the frequency of the forcing term is well within the system bandwidth $\tau^{-1}$, then the device essentially behaves like a static nonlinearity (with the left-hand side of (1) equated to zero) and the system output follows the dynamic of the forcing signal. As the input field traverses two thresholds, given essentially by the inflection points of the potential (2), the system commutes from one state to the other, following the nonlinear trajectory leading to the hysteretic behavior [6].

In the following discussion, as a dc magnetic field is the target of interest to be detected, the device will be treated as a static nonlinearity, assuming that the dynamic of the magnetic core is negligible compared to the forcing field frequency (which anyway must assure the coupling between the primary and secondary coils).

## The RTD Fluxgate Idea

The RTD fluxgate, developed at the DIEES laboratory in Catania, Italy, in collaboration with researchers from the SPAWAR System Center, San Diego, California, is based on a two-coil structure (primary and secondary) wound around a suitable magnetic core having a hysteretic input-output characteristic.

The basic idea is that the magnetic core has two switching thresholds and a two-state output, whose behavior can be described via the double-well potential energy function, $U(m,t)$ [1]–[3]. To reverse the core magnetization (from one steady state to the other), the driving field $(H(t) = H_e + H_x)$ must cross the switching thresholds. With a

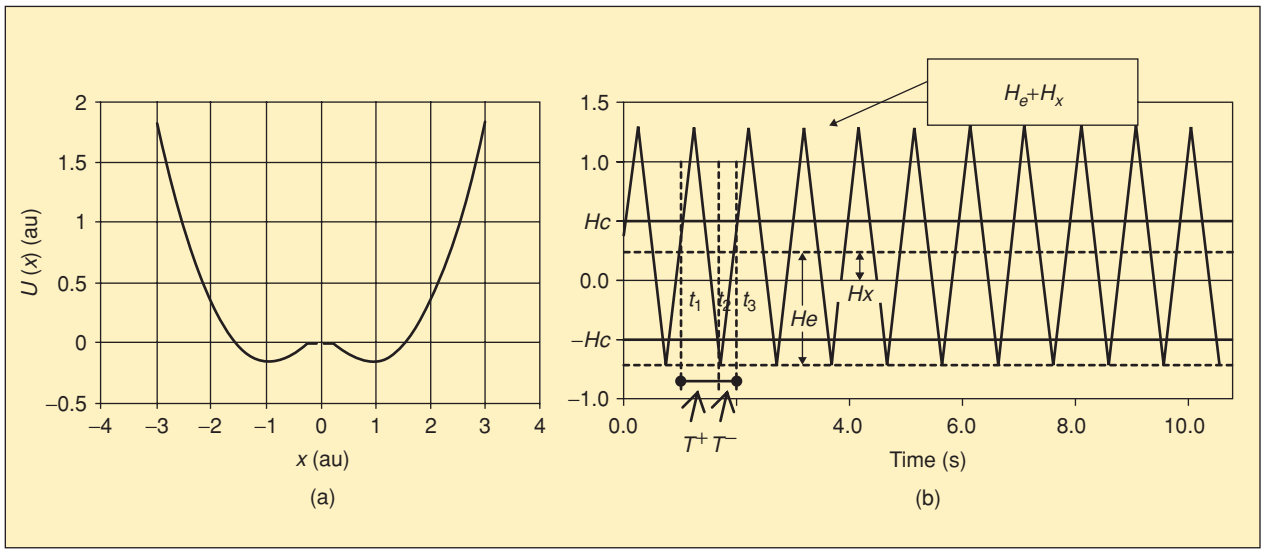


*Fig. 2.* (a) Potential energy function that describes the evolution over the time of the core magnetization. (b) Schematic representation of the switching events in the case of a triangular excitation field with a superimposed dc target field.

time-periodic excitation, $H_e$, having an amplitude just sufficient to cause switching between the steady states in the absence of the target field, the hysteresis loop (or the underlying potential energy function $U(m, t)$) is symmetric and two identical residence times (defined as the time of residence in one of the stable steady states of the core) are obtained leading to a zero RTD. Then, the presence of the dc target signal ($H_x$) leads to a skewing of the hysteresis loop with a direct effect on the residence times; they are no longer the same [6]. Figure 2(b) shows this situation for a triangular excitation superimposed on an external dc field. It is observed that the crossing events (when $H_e + H_x$ reaches the switching thresholds of the hysteretic core) define two different residence times, so that $RTD \neq 0$. The TD value depends on the target field.

A very simple sensor structure, negligible onboard power requirements, and the intrinsic digital form of the readout signal are the main advantages of the proposed strategy over the conventional fluxgate. These statements will be discussed in the following, where the need to operate at low frequency values (in the range 30–100 Hz) and low excitation signal amplitudes to obtain high sensitivity is highlighted. This is a very important feature for practical applications, contrary to conventional fluxgates, which require large excitations to improve the quality of the output signals.

Moreover, as discussed later, these detectors are characterized by high sensitivity, suitable resolution, and low noise floor comparable to that of marketed devices.

In the case of triangular excitation, the following expression for the device sensitivity was obtained [1], [2]:

$$S_{\text{Tria}} = \frac{\partial \text{RTD}}{\partial H_x} = \frac{2\pi}{\omega \hat{H}_e}, \tag{3}$$

$\hat{H}_e$ and $\omega$ being the amplitude and the frequency of the excitation field, respectively. It must be highlighted that the following condition must be fulfilled to assure the system switching:

$$\hat{H}_e \geq H_x + H_c, \tag{4}$$

with $H_c$ being the coercive field of the magnetic core.

These expressions were obtained under the hypothesis of a static soft magnetic core that rapidly saturates as the forcing field level reaches the coercive field, which is consistent with RTD theory [6] and the magnetic core adopted to develop the prototype under investigation (see "An Experimental Prototype"). The behavior of $S_{\text{Tria}}$ as a function of the frequency and the amplitude of the excitation field is shown in Figure 3(a). As expected, with a triangular excitation the sensitivity does not depend on the target magnetic field amplitude, thereby allowing very simple processing of the output signal. Moreover, the sensitivity of the device increases as the excitation frequency and amplitude decrease, thus allowing optimization of the onboard power requirements.

In the case of a sinusoidal excitation, the following expression of the device sensitivity is obtained [1], [2]:

$$S_{\text{Sin}} = \frac{\partial \text{RTD}}{\partial H_x} = \frac{2}{\omega}\left[\frac{\frac{1}{\hat{H}_e}}{\sqrt{1-\left(\frac{H_c+H_x}{\hat{H}_e}\right)^2}} + \frac{\frac{1}{\hat{H}_e}}{\sqrt{1-\left(\frac{H_c-H_x}{\hat{H}_e}\right)^2}}\right]. \tag{5}$$

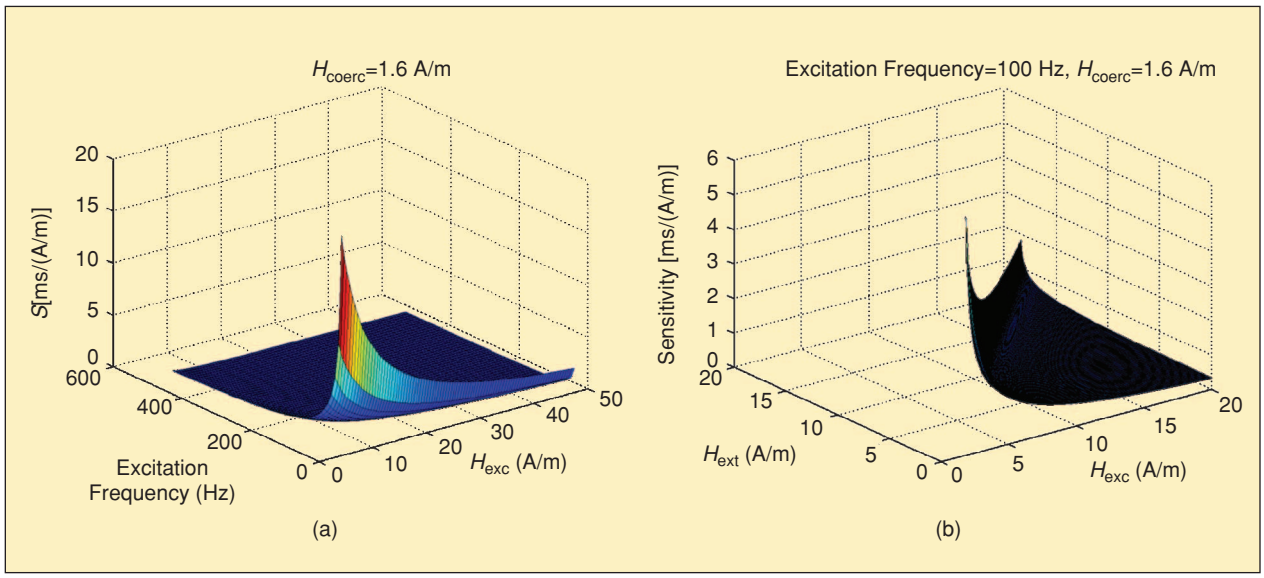


*Fig. 3.* Sensitivity in the case of (a) a triangular excitation and (b) a sinusoidal excitation.

The form of $S_{\mathrm{Sin}}$ displays its dependence on both the amplitude and frequency of the excitation and on the dc target signal level, $H_x$. The behavior of $S_{\mathrm{Sin}}$ in the case of sinusoidal bias is sketched in Figure 3(b). As can be observed, the device sensitivity increases as $\hat{H}_e$ decreases [of course, as already discussed, the amplitude of the excitation must fulfill condition (4)]. At the same time $S_{\mathrm{Sin}}$ increases with $H_x$ due to the variation in the excitation slope corresponding to the crossing event times. The latter behavior becomes evident when $\hat{H}_e = H_x + H_c$.

Figure 4 shows a comparison between sensitivities in the case of a triangular excitation (circles) and a sinusoidal excitation (solid lines) as a function of the excitation amplitude, for several target signal values (each sensitivity curve has been calculated for a fixed value of $H_x$). The results highlight that the sensitivity curves, with the sinusoidal excitation, will diverge in the limit set by (4) and represented by the limiting excitation curves (the vertical dotted lines in the graph background).

As an example, with $H_x = 2.2$ A/m (with $H_c = 1.6$ A/m), the bound for the excitation is 3.8 A/m (obtained by computing $H_c + H_x$), as evidenced by the bold vertical line in Figure 4. These bounds represent the minimum excitation value to assure switching events for the target and coercive field considered values. In conclusion, it can be stated that the use of a sinusoidal excitation, implying undesirable dependence of the sensitivity on the target signal, is valuable when driving the device at the switching threshold, as compared with triangular excitation.

The latter consideration allows us to state that if the operating range of the sensor lies in a small interval (so that the limit condition $H_e = H_x + H_c$ is roughly satisfied for each target field belonging to the operating range) sinusoidal excitation will perform better than the triangular excitation.

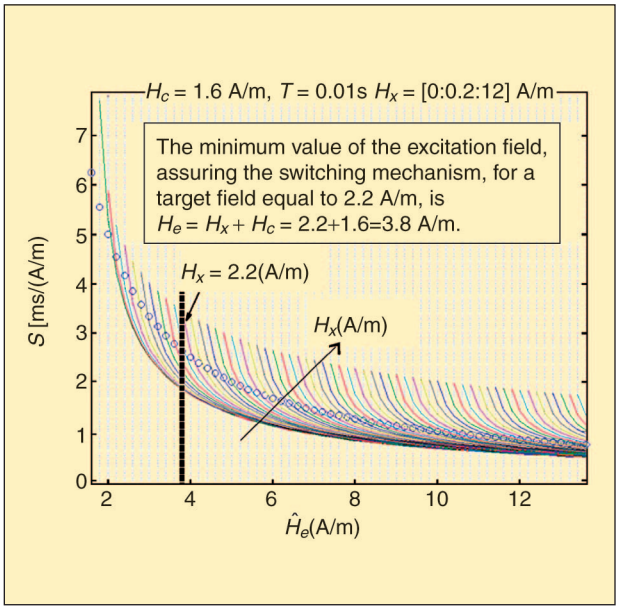


***Fig. 4.*** Comparison between sensitivity in the case of a triangular bias and a sinusoidal bias as a function of the bias amplitude, for several values of the target signal (each sensitivity curve corresponds to a fixed target signal). Two different regions are evidenced for each value of the target field, which are defined by the intersection between the sensitivity curve for the triangular bias (circle) and the sensitivity curve for the sinusoidal bias corresponding to the considered target signal: a region where the sinusoidal bias gives a best sensitivity and a region where the triangular bias dominates. This behavior is consistent with the above consideration on the sensitivity burst very close to the limit region of commutation (defined by $H_e = H_c + H_x$). In fact, sensitivity in the case of the sinusoidal bias will diverge in this limit of operation. In the graph the bound bias curves are also given (the vertical lines in the graph background); each curve is related to one sensitivity curve and represents the minimum value of the bias signal ($H_e$) driving the system into commutation (the commutation limit) when the target signal amplitude ($H_x$) assumes value for which each sensitivity curve has been calculated.

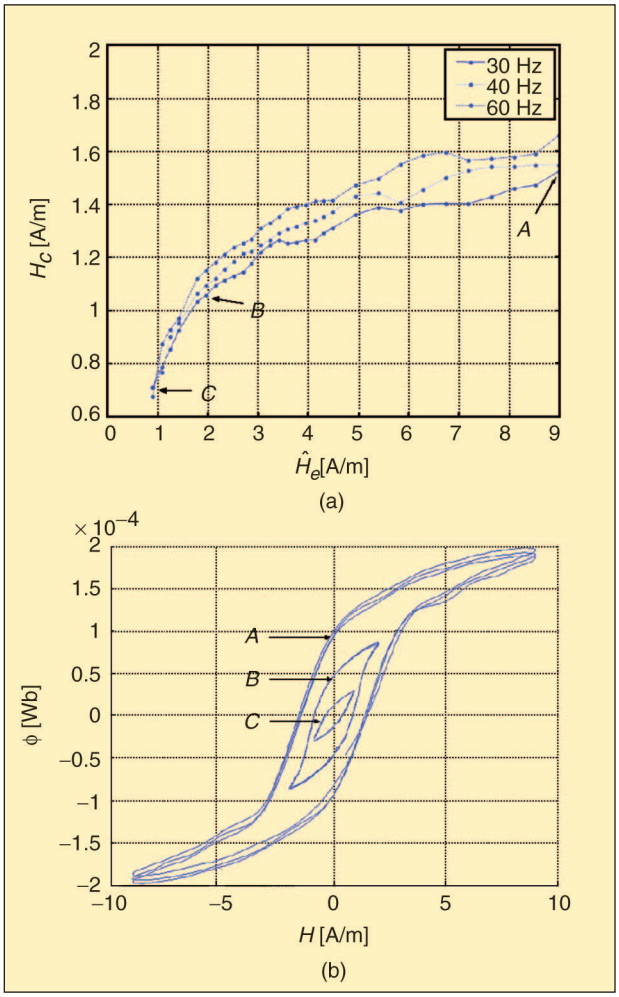


***Fig. 5.*** (a) Behavior of $H_c$ as function of excitation amplitude. The points A, B, and C indicate where the hysteresis cycles were computed; (b) experimental hysteresis cycles (A,B,C) obtained for three values of excitation (sinusoidal) field.

## Quantities Affecting the RTD Fluxgate Performances

Influencing quantities, such as magnetic noise or electric noise, perturb the behavior of the RTD fluxgate. In particular, the following indexes can be adopted to assess the effects of noise on the performance of the device:

- noise floor
- resolution in terms of the minimum amplitude of $H_x$, which can be detected
- uncertainty in the estimation of the RTD
- uncertainty in the estimation of the target field, $H_x$.

As procedures for the estimation of these quantities are well known in the literature, we will focus on the main contributions affecting these indexes and possible solutions.

Magnetic noise, electric noise, and poor magnetic coupling leading to badly defined spiking output are the main contributions to the quantities defined above. Moreover, uncertainty introduced by the model relating the measured RTD to the target field $H_x$ must be taken into account to evaluate the uncertainty of $H_x$. To reduce these effects, the following suggestions could be taken into account during design of the device:

- reduce electric noise in the driving signal by using suitable shielding strategies
- reduce the effect of noise (superimposed on the output signal) on the performance of the readout electronics (e.g., a Schmitt Trigger to estimate the crossing events) by increasing the frequency and the amplitude of the bias field (although this clashes with a high level of sensitivity)
- reduce the effect of a poorly defined spiking output on the estimation of the RTD by improving the magnetic coupling; as an example, a suitable choice of the magnetic core material would lead to better coupling and a valuable output signal
- make uncertainty in readout electronics negligible as compared to other contributions
- if applicable, including post-processing sections to filter out the noise. If, during the design, the effects of electric noise and bad magnetic coupling are made negligible compared to the other causes, all the device indexes addressed above could be considered as only depending on magnetic noise.

## Considerations on the Design of an RTD Fluxgate

During the design of an RTD fluxgate, several choices must be made, including the technology, the topology of the core, and the selection of a suitable magnetic material. Moreover, the operating conditions have to be defined, allowing the required specifics in terms of power

**Table 1. Magnetic materials adopted for the magnetic core.**

| Material | $H_c(A/m)$ |
|---|---|
| 2714A as cast | 1.6 |
| 2714A annealed | 0.16 |
| 2705A as cast | 1.12 |

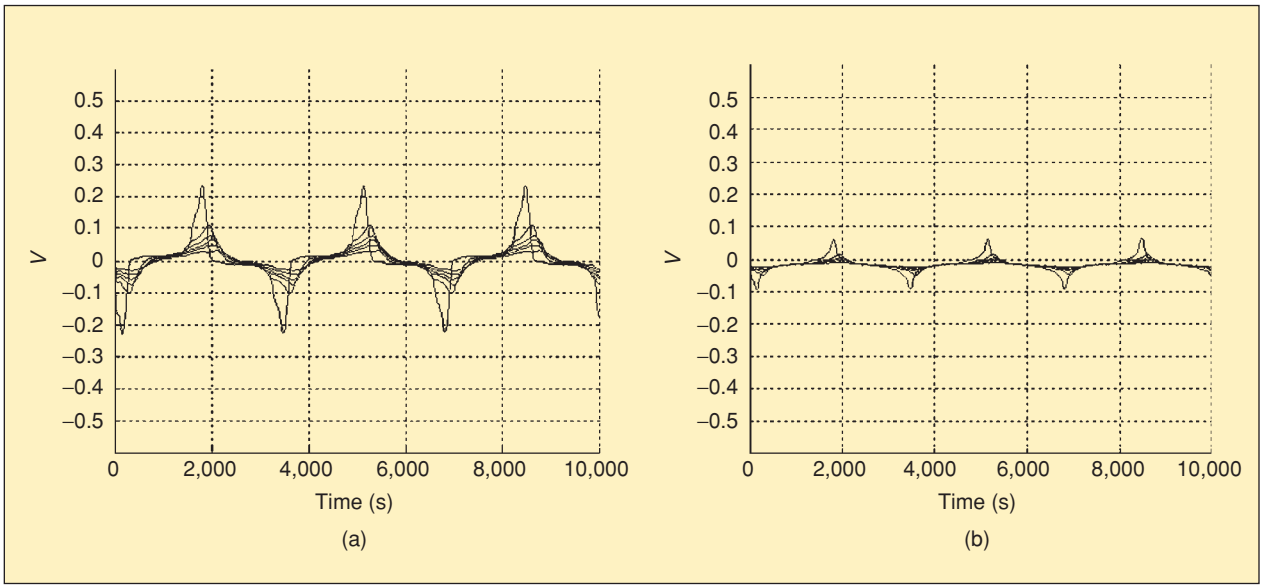


*Fig. 6.* Output voltages at the pick up coils by using (a) the 2705A core, as cast; (b) 2714A core, as cast. Curves are for excitation fields of amplitude: 3.5908 A/m, 1.7954 A/m, 1.4363 A/m, 1.2567 A/m, 1.0772 A/m, 0.8977 A/m.

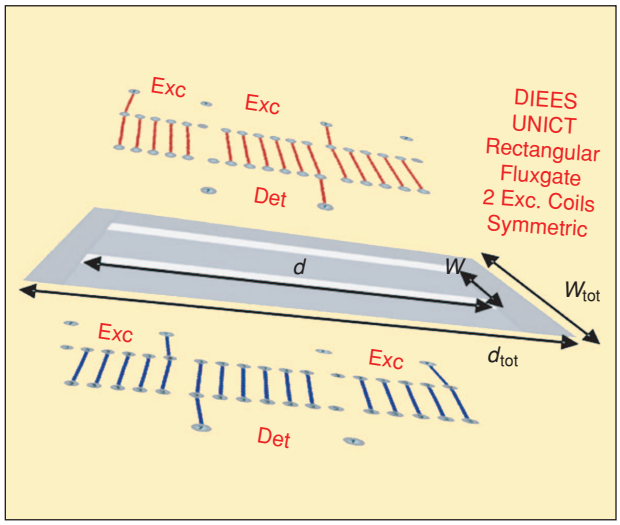


*Fig. 7.* PCB layout of the RTD fluxgate.

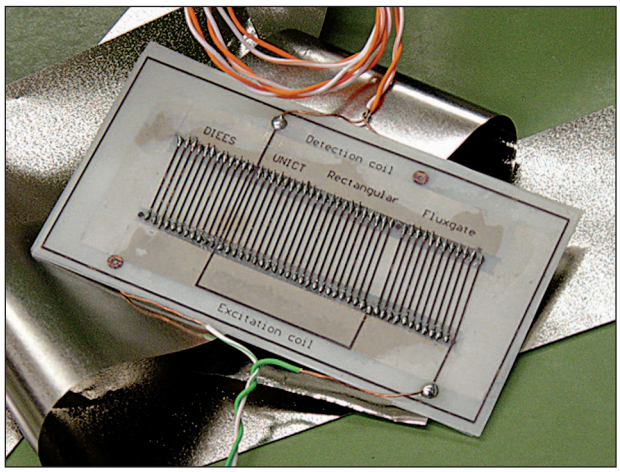


*Fig. 8.* RTD fluxgate prototype and a sample of magnetic alloy 2714A.

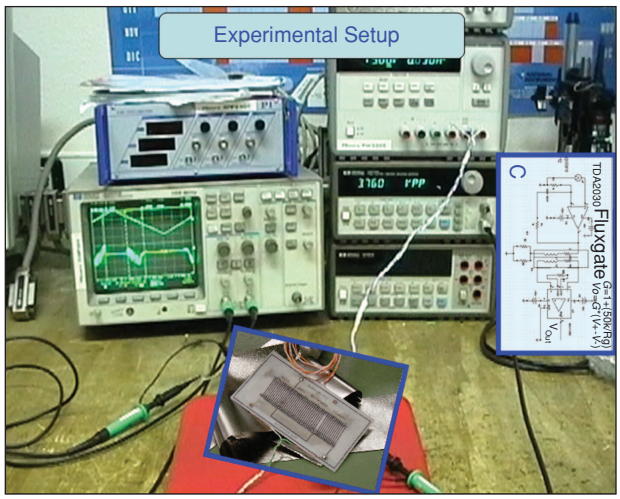


*Fig. 9.* Experimental set-up to operate and test the PCB RTD fluxgate.

consumption, resolution, sensitivity, noise floor, and operating range to be met. Covering all these aspects is beyond the scope of this general discussion, but some interesting considerations on how to fix the operating conditions so as to optimize the tradeoff between a suitable spiking output (obtained with a high forcing field amplitude), power requirements, and high sensitivity (requiring a low excitation field) will be given. Moreover, some criteria for the selection of the core material are discussed.

The dependence of the hysteresis cycle on the bias signal amplitude and frequency is well known [10]. Figure 5(a) shows the behavior of the coercive field as a function of the forcing field amplitude for the prototype. Figure 5(b) depicts the hysteresis cycles obtained with three (sinusoidal) excitation field amplitudes (1 A/m, 2 A/m, 9 A/m) corresponding to points A, B, C in Figure 5(a). As can be observed, reducing the forcing field produces

- hysteretic loops that are no longer sharp (curve C) leading to a badly spiking output signal, which affects the RTD readout strategy
- a sharp reduction in the coercive field, which is not consistent with the possibility of working at the limit (4) ($H_e = H_c + H_x$), represents the theoretical regime of maximal sensitivity.

A suitable tradeoff between power requirements, sensitivity, and reliability of the readout strategy (well defined spiking output) must be assured. As an example, the operating conditions indicated with the arrow B seem to represent the lower bound of the forcing field amplitude allowing the device to operate with a sharp characteristic and a coercive field weakly dependent on the driving field. The choice of a suitable material for the ferromagnetic core gives the possibility to improve the features of the device even further. Investigations into magnetic materials belonging to the METGLAS alloys family and shown in Table 1 were performed in [2]. One criterion for selection of the most suitable material could be to fulfill conditions allowing the device to operate in the region of maximum sensitivity in the sense of (4), for a given small operating range [2].

At the same time, a material assuring a well-defined spiking voltage at the pickup coil could be much more valuable than materials showing any other features. As an example, Figure 6 shows responses of RTD fluxgate prototypes using the 2705A and the 2714A cores. As can be observed, the sharp hysteresis of material 2705A allows the device to produce output signals performing better than the 2714 as cast. This offers the opportunity to decrease the value of the bias amplitude (increasing the sensitivity and reducing the power demand) or improve the performance of the readout strategy (in terms of reliability in RTD computation).

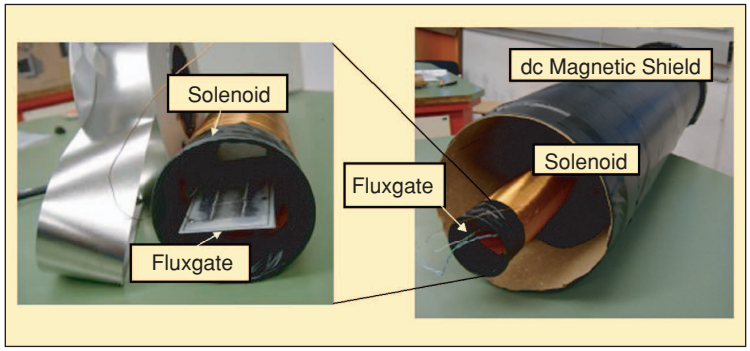


*Fig. 10.* A view of the characterization chamber used to force the target field on the RTD fluxgate during the device characterization.

**Table 2. Performances of the experimental prototype, realized in PCB technology and using the 2714A (cobalt-based) magnetic core, by Metglass Solutions.**

| | |
|---|---|
| Resolution $\left(\delta H_x^{\mathrm{EXT}}\right)$ | 1nT |
| Best sensitivity $\left(\frac{\partial \mathrm{RTD}}{\partial H_x^{\mathrm{INT}}}\right)$ | 20ms/$\mu$T |
| Demagnetizing factor $\left(\frac{H_x^{\mathrm{EXT}}}{H_x^{\mathrm{INT}}}\right)$ | 40 |
| Noisefloor | $\frac{20\mathrm{pT}}{\sqrt{(\mathrm{Hz})}}$ |
| Power consumption | 1mW |

## An Experimental Prototype

In the literature, there are many examples of fluxgate magnetometers developed using different technologies, from printed circuit board (PCB) technology to the standard CMOS approach [8], [9], [12], [15], [16], [22]. In this section, some notes about an RTD fluxgate sensor developed in our laboratories by a standard PCB technology are given [1], [2].

The device is made up of three layers, as shown in Figure 7. The as-cast magnetic alloy 2714A (cobalt-based), by Metglass Solutions, was adopted for its very sharp characteristic. Figure 8 shows the RTD fluxgate prototype and a sample of the magnetic core. The important parameters of the adopted core are its coercive field, $H_c = 1.6$ A/m, and the dc permeability $\mu > 80,000$.

Figure 9 shows the setup adopted to test the device, which uses a digital scope, an arbitrary waveform generator, and dedicated electronics to perform signal conditioning.

Figure 10 is a view of the characterization chamber adopted to force a known magnetic field on the device.

Figures 11 and 12 show a comparison between the predicted sensitivity and the experimental behavior in the case of a sinusoidal and triangular bias, respectively. It must be observed that sensitivities are estimated as the ratio between the RTD variation and the corresponding variation of the magnetic field inside the device. The latter was estimated by postprocessing input/output signals [1].

By analyzing the results, the predicted reduction in sensitivity with increasing amplitudes and forcing term frequencies emerges. The results clearly show that the predicted

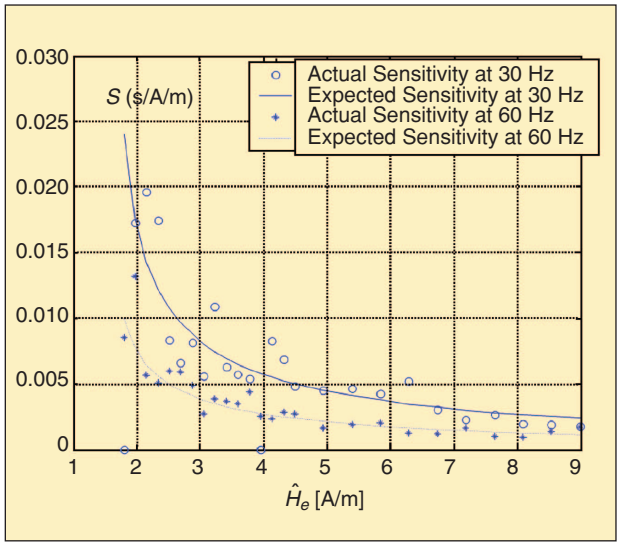


*Fig. 11.* Comparison between expected and actual sensitivities at 30 Hz and 60 Hz (sinusoidal excitation); the sensitivity has been computed over a variation of the target field of $\Delta H_x = 0.155$ A/m.

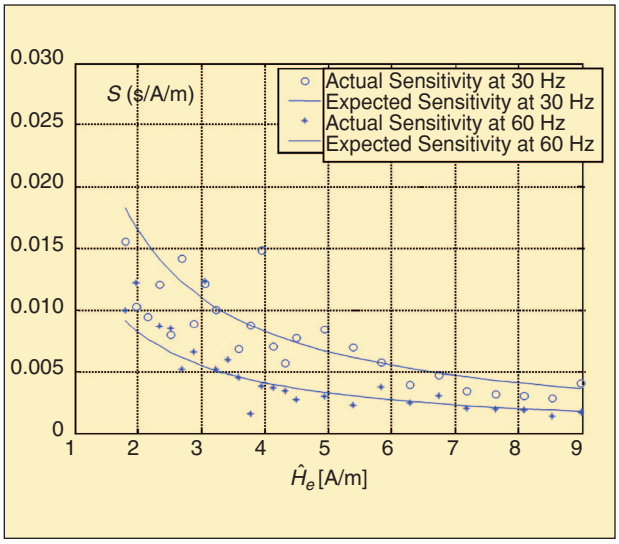


*Fig. 12.* Comparison between expected and actual sensitivities at 30Hz and 60 Hz (triangular excitation); the sensitivity has been computed over a variation of the target field of $\Delta H_x = 0.155$ A/m.

behavior suitably fits the observed behavior; however, modifications in the nominal behavior of the coercive field due to the reduction in the driving amplitude perturb the behavior of the device with very low forcing fields.

Table 2 summarizes the other performance of the sensor operating with a sinusoidal excitation field. The resolution obtained (estimated as the minimum external magnetic field detectable with the device), the demagnetization factor (calculated by measuring the external field imposed on the device and estimating the internal field by post-processing the acquired input-output waveforms), and the noise floor are comparable to those of a conventional device, making these sensor very promising devices, due to their simplicity and the other advantages highlighted in this article. Moreover, as the target to be detected is a dc magnetic field, an average operator can be applied over several periods of the output waveform to improve the resolution and the noise floor performance.

## Acknowledgment

We gratefully acknowledge support from the U.S. Office of Naval Research, Code 331.

## References

[1] B. Andò, S. Baglio, A.R. Bulsara, and V. Sacco, "Effects of driving mode on RTD-Fluxgate performances," in *Proc. IEEE Instrumentation Measurement Tech. Conf. (IEEE IMTC2004)*, Como, Italy, 2004, vol. 2, pp. 1419–1423.

[2] B. Andò, S. Baglio, A.R. Bulsara, and V. Sacco, "Investigation on optimal materials selection in RTD-Fluxgate Design," in *Proc. IEEE Instrumentation Measurement Tech. Conf. (IEEE IMTC2005)*, Ottawa, Canada, 2005, pp. 1261–1265.

[3] S. Baglio, V. Sacco, A. Bulsara, and P. Nouet, "Read-out circuit in RT-Fluxgate," in *Proc. Int. Simp. Circuits Systems*, Kobe, Japan, 2005, pp. 5910–5913.

[4] R. Banning, W.L. de Koning, H. J.M.T.A. Adriaens, and R.K. Koops, "State-space analysis and identification for a class of hysteretic systems," *Automatica*, vol. 37, no. 12, pp. 1883–1892, 2001.

[5] W. Bornhofft and G. Trenkler, *Sensors, a Comprehensive Survey*, W. Gopel, J. Hesse, and J. Zemel, Eds. New York: VCH 1989.

[6] R. Bulsara, C. Seberino, and L. Gammaitoni, "Signal detection via residence-time asymmetry in noisy bistable devices," *Phys. Rev. E*, vol. 67, no. 1, pp. 016120–016121, 2003.

[7] K. Chakrabarti and M. Acharyya, "Dynamic transition and hysteresis," *Rev. Mod. Phys.*, vol. 71, no. 3, pp. 847–859, 1999.

[8] L. Chiesi, P. Kejik, B. Janossy, and R.S. Popovic, "CMOS planar 2D micro-fluxgate sensor," *Sens. Actuators A, Phys.*, vol. 82, no. 1-3, pp. 174–180, 2000.

[9] O. Dezuari, E. Belloy, S.E. Gilbert, and M.A.M. Gijs, "Printed circuit board integrated fluxgate sensor," *Sens. Actuators A, Phys.*, vol. 81, no. 1-3, pp. 200–203, 2000.

[10] K. Enpuku, D. Kuroda, A. Ohba, T.Q. Yang, K. Yoshinaga, T. Nakahara, H. Kuma, and N. Hamasaki, "Biological immunoassay utilizing magnetic marker and high tc superconducting quantum interference device magnetometer," *Jpn. J. Appl. Phys., pt. 2*, vol. 42, no. 12, pp. L 1436–L 1438, 2003.

[11] F. Forster, "A method for the measurement of dc field differences and its application to nondestructive testing," *Nondestr. Test*, vol. 13, pp. 31–41, 1955.

[12] R. Gottfried, W. Budde, and S. Ulbricht, "A miniaturized magnetic field sensor system consisting of a planar fluxgate sensor and a CMOS readout circuitry," in *Proc. Transducers'95-Eurosensors IX 289–A 12*, pp. 229–232

[13] P. Jung, G. Gray, and R. Roy, "Scaling law for dynamical hysteresis," *Phys. Rev. Lett.*, vol. 65, no. 15, pp. 1873–1876, 1990.

[14] F. Kaluza, A. Gruger, and H. Gruger, "New and future applications of fluxgate sensors," *Sens Actuators A, Phys.*, vol. 106, no. 1-3, pp. 48–51, 2003.

[15] S. Kawahito, C. Maier, M. Schneider, M. Zimmermann, and H. Baltes, "A 2-D CMOS microfluxgate sensor system for digital detection of weak magnetic fields," *IEEE J. Solid-State Circuits*, vol. 34, no. 12, p. 1843, 1999.

[16] P. Kejık, L. Chiesi, B. Janossy, and R.S. Popovic, "A new compact 2D planar fluxgate sensor with amorphous metal core," *Sens. Actuators A, Phys.*, vol. 81, no. 1-3, pp. 180–183, 2000.

[17] R.H. Koch and J.R. Rozen, "Low-noise flux-gate magnetic-field sensors using ring-and rod-core geometries," *Appl. Phys. Lett.* 78, vol. 13, pp. 1897–1899, Mar. 2001.

[18] F. Primdahl, "The fluxgate mechanism, part 1: the gating curves of parallel and orthogonal fluxgates," *IEEE Trans. Magn.*, vol. 6, no. 2, pp. 376–383, 1970.

[19] H. Richter, E.A. Misawa, D.A. Lucca, and H. Lu, "Modelling nonlinear behavior in a piezoelectric actuator," *Precision Eng.*, vol. 25, pp. 128–137, 2001.

[20] P. Ripka, *Magnetic Sensors and Magnetometers.* Boston, MA: Artech, 2001.

[21] S. Sivasubramanian, A. Widom, and Y. Srivastava, "Equivalent circuit and simulations for the landau-khalatnikov model of ferroelectric hysteresis," *IEEE Trans. Ultrason., Ferroelect. Freq. Contr.*, vol. 50, no. 8, pp. 950–957, 2003.

[22] A. Tipek, P. Ripka, T. O'Donnell, and J. Kubik, "PCB technology used in fluxgate sensor construction," *Sens. Actuators A, Phys.*, vol. 115, no. 2-3, pp. 286–292, 2004.

***Bruno Andò*** (bruno.ando@diees.unict.it) received the degree in electronic engineering from the University of Catania, Italy, in 1994 and a Ph.D. degree in 1999. Since 1999, he worked as a researcher with the Electrical and Electronic Measurement Group of the University of Catania—DEES, where, in 2002, he became an assistant professor. His primary research interests are sensors design and optimization.

*(continued on page 73)*

electricity shortages, which culminated in massive shortages during the early 2000s.

### Imperfect Crystal Ball

A careful reading of Joe Keithley's book illustrates that throughout the period covered by this book, no seer could predict the future. Scientific knowledge is increasing and spreading. Measurement certainties have improved. Photonics, also referred to as lightwave technologies, show evidence of becoming an increasingly important technology that could supersede and complement electronics in the future. Extrapolation, though, may be deceptive.

***Bernie Gollomp*** (b.gollomp@ieee.org) has spent four decades in industry during which he received two AlliedSignal Technical Achievement awards and issued many patents. He drafted the IEEE Society constitution and bylaws and AUTOTESTCON IEEE charter. An IMTC founder, he drafted the IMTC IEEE charter and helped launch the first two conferences. He is an IEEE Life Fellow.



## instrumentationnotes *continued from page 71*

***Salvatore Baglio*** received the "Laurea" and the Ph.D. degree from the University of Catania in 1990 and 1994 respectively. Since 1996 he has been with the Dipartimento di Ingegneria Elettrica Elettronica e dei Sistemi of the University of Catania where he is an associate professor. He was associate editor for *IEEE Transactions on Circuits and Systems* and a Distinguished Lecturer for the IEEE Circuits and System Society. His research interests are in measurement methodologies and smart sensors.

***Adi R. Bulsara*** received his Ph.D. in physics from the University of Texas, Austin, in 1978. He is now a senior researchers at the U.S. Navy Space and Naval Warfare Systems Center, in San Diego, where he heads a group that specializes in applications of nonlinear dynamics. He is a Fellow of the American Physical Society. His primary research interests are in the physics of noisy nonlinear dynamic systems.

***Vincenzo Sacco*** received the M.S. in electronic engineering in 2002. In 2003 he was an assistant researcher at Leeds University. He is currently in Ph.D. program in electronic and automation engineering at the University of Catania. His research interests are in technology for integrated sensors and exploitation of nonlinearity for sensing application.